Journal of Catalysis **186,** 325–333 (1999)
Article ID jcat.1999.2510, available online at http://www.idealibrary.com on IDEAL®

Isotopic Tracer and Kinetic Studies of Oxidative Dehydrogenation Pathways on Vanadium Oxide Catalysts

Kaidong Chen, Andrei Khodakov, Jun Yang, Alexis T. Bell,[1] and Enrique Iglesia[1]

Chemical and Materials Sciences Divisions, Lawrence Berkeley National Laboratory, and Department of Chemical Engineering,
University of California, Berkeley, California 94720-1462

Received January 27, 1999; accepted March 30, 1999

Kinetic analysis and isotopic tracer studies were used to identify elementary steps and their reversibility in the oxidative dehydrogenation of propane on VO_x/ZrO_2 catalysts with VO_x surface densities between 1.6 and 6 VO_x/nm^2. Competitive reactions of C_3H_6 and $CH_3{}^{13}CH_2CH_3$ showed that CO forms via secondary combustion of propene intermediates. CO_2 formed via this reaction and also via the direct combustion of propane. Reactions of $^{18}O_2/C_3H_8$ mixtures on supported $V_2{}^{16}O_5$ led to the preferential initial appearance of lattice ^{16}O atoms in all oxygen-containing products, as expected if lattice oxygens were required for the activation of C–H bonds. Isotopically mixed O_2 species were not detected during reactions of C_3H_8–$^{18}O_2$–$^{16}O_2$ reactant mixtures. Therefore, dissociative O_2 chemisorption steps are irreversible. Similarly, C_3H_8–C_3D_8–O_2 reactants undergo oxidative dehydrogenation without forming $C_3H_{8-x}D_x$ mixed isotopomers, suggesting that C–H bond activation steps are also irreversible. Normal kinetic isotopic effects ($k_{C–H}/k_{C–D} = 2.5$) were measured for primary oxidative dehydrogenation reactions. Kinetic isotope effects were slightly lower for propane and propene combustion steps (1.7 and 2.2, respectively). These data are consistent with kinetically relevant steps involving the dissociation of C–H bonds in propane and propene. C_3H_6–D_2O and C_3D_6–H_2O cross exchange reactions occur readily during reaction; therefore, OH recombination steps are reversible and nearly equilibrated. These isotopic tracer results are consistent with a Mars–van Krevelen redox mechanism involving two lattice oxygens in irreversible C–H bond activation steps. The resulting alkyl species desorb as propene and the remaining O–H group recombines with neighboring OH groups to form water and reduced V centers. These reduced V centers reoxidize by irreversible dissociative chemisorption of O_2. The application of pseudo-steady-state and reversibility assumptions leads to a complex kinetic rate expression that describes accurately the observed water inhibition effects and the kinetic orders in propane and oxygen when surface oxygen and OH groups are assumed to be the most abundant surface intermediates. © 1999 Academic Press

1. INTRODUCTION

Catalytic dehydrogenation is currently used to convert alkanes to alkenes, but it is an endothermic process that requires high temperatures. Pyrolysis and cracking side reactions lead to high methane and carbon yields. Oxidative dehydrogenation (ODH) provides a potential alternate route to alkenes; it is an exothermic reaction and the presence of O_2 inhibits carbon deposition. These advantages have led to many studies of the reaction pathways and of the structure of the most selective catalysts for oxidative dehydrogenation of propane (1–7), with the ultimate objective of minimizing combustion side reactions that limit propene yield to less than 30%.

Kinetic rate expressions for oxidative dehydrogenation and combustion pathways can provide mechanistic suggestions for these reactions, but they are insufficient to establish the identity and reversibility of individual surface elementary steps. Transient and steady-state isotopic studies can discriminate among various mechanistic proposals that may be consistent with measured kinetic rate expressions. Such studies can also confirm the assumptions required in order to obtain a given rate expression from a sequence of elementary steps. Many studies of the synthesis, characterization, and reactivity of ODH catalysts have addressed only indirectly the details of the primary and secondary reactions occurring during ODH of light alkanes (8–14). By analogy with other oxidation reactions, the reaction has been proposed to proceed via a Mars–van Krevelen redox sequence (8, 11–13), in which alkanes react with lattice oxygen and the resulting vacancies react with dissociatively adsorbed O_2. These mechanistic proposals have been largely based on agreement between proposed sequences of elementary steps and experimental power-law kinetic rate expressions, with limited independent evidence for specific elementary steps (12).

Catalysts based on supported vanadia are among the most active and selective oxidative dehydrogenation catalysts (7). Polyvanadate structures supported on ZrO_2 provide an optimum compromise between the reducibility and the accessibility of VO_x domains and lead to more active catalysts than VO_x dispersed on other supports (4). Catalytic studies show that highly dispersed polyvanadates exhibit ODH turnover rates similar to those of bulk V_2O_5 (4, 5). On VO_x/ZrO_2, the highest specific activity (per total

---

[1] To whom correspondence should be addressed. E-mail: iglesia@cchem.berkeley.edu; bell@cchem.berkeley.edu.

0021-9517/99 $30.00

V atom) was reached for surface densities of 3–4 VO_x/nm^2, and the initial (zero-conversion) propene selectivities were about 80–85% (605 K, 14 kPa C_3H_8, 1.7 kPa O_2) (5). A kinetic analysis of primary and secondary reaction pathways showed that the relative rates of propane dehydrogenation and propene combustion do not depend on the structure or surface density of VO_x species on any of the supports studied (4, 5).

The objective of this study is to determine the identity and reversibility of elementary steps involved in the ODH reactions of propane, to establish the identity of kinetically relevant intermediates, and to infer the nature of the active surface species required to catalyze the rate-determining elementary steps. Isotopic tracer methods were combined with measurements of the concentration dependence of individual reaction rates. Most of the data were obtained on VO_x/ZrO_2 catalysts having VO_x densities between 1.6 and 6.0 VO_x/nm^2. The kinetics of propane ODH were also determined for bulk V_2O_5 in order to provide a comparison with VO_x/ZrO_2 catalysts.

2. EXPERIMENTAL

VO_x/ZrO_2 catalysts (4, 10, and 15 wt% V_2O_5) were prepared by incipient wetness impregnation of precipitated zirconium oxyhydroxide powders with solutions of ammonium metavanadate (99%, Aldrich, Inc.) (5). Impregnated samples were dried overnight in ambient air at 393 K and then treated in dry air at 773 K for 4 h.

Reaction rate measurements were carried out in a packed-bed quartz microreactor with plug-flow hydrodynamics (5). C_3H_8 and O_2 conversions were varied by changing reactant flow rates between 50 and 200 cm^3/min. Typical propane conversions were less than 1% and oxygen conversions were below 20%. Reaction rates were extrapolated to zero residence time in order to obtain initial reaction rates. Water was added to the C_3H_8–O_2 feed by flowing a 20% H_2/Ar mixture through a CuO bed (0.5 m long, 150 g CuO) held at 623 K. Water was formed by the reduction of CuO to Cu metal. All transfer lines located downstream of the point of water introduction were kept above 393 K in order to prevent condensation.

$^{18}O_2$ isotopic tracer studies were performed in a packed-bed single-pass flow microreactor with plug-flow hydrodynamics. Samples were placed in the quartz reactor, treated in 5% $^{16}O_2$/95% He at 773 K for 1 h, and cooled to room temperature. The 5% $^{16}O_2$/95% He mixture was then switched to $^{16}O_2/^{18}O_2$/He/Ar/C_3H_8 (0.9% $^{16}O_2$, 0.9% $^{18}O_2$, 15.4% C_3H_8, 1% Ar, He balance) or $^{18}O_2$/He/Ar/C_3H_8 (1.8% $^{18}O_2$, 15.4% C_3H_8, 1% Ar, He balance) at a flow rate of 1.67 cm^3 s^{-1}. After 1 h, the temperature was increased from ambient to 873 K at 0.33 K s^{-1}. The chemical and isotopic compositions of the reactor effluent were measured by online mass spectrometry (Leybold Inficon, Transpector RCA 200) at 6 s intervals. Ar was used as an internal standard in order to determine the absolute concentrations of reactants and products.

Deuterium and ^{13}C isotopic tracer studies were carried out in a gradientless batch reactor containing a shallow packed-bed within a gas recirculation loop (15). Reactants and products were recirculated at 3.3 cm^3 s^{-1} using a graphite gear micropump in order to maintain differential reactor conditions (<1% propane conversion per pass). The reactor was evacuated by mechanical and diffusion pumps isolated from the system by liquid nitrogen traps. The chemical and isotopic compositions of reactants and products were measured by a GC-MS (Hewlett–Packard 5972). The deuterium and carbon-13 contents in the products were determined from mass spectrometric data using matrix techniques that correct for ion fragmentation and natural ^{13}C abundance (16).

Undeuterated propane (Matheson, instrument purity, >99.5%), perdeuterated propane (Isotec, chemical purity >99.0%, isotopic purity >99.0%), [2-^{13}C]propane (Cambridge Isotopes, chemical purity >98.0%, isotopic purity >99.0%), oxygen (research grade, >99.999%), and propene (Matheson, C.P., >99.0%) were used as reactants without further purification. Perdeuterated water (D_2O; Isotec, chemical purity >99.0%, isotopic purity >99.0%) and distilled water (H_2O) were purified by several freeze–thaw evacuation cycles before use. Helium (Research grade, >99.999%) was used as an inert diluent in all studies.

3. RESULTS AND DISCUSSION

3.1. Reaction Network

The oxidation of propane on VO_x/ZrO_2 occurs via parallel and sequential steps, as shown in Scheme 1 (1). Propene forms as a primary product of oxidative dehydrogenation and carbon oxides (CO_x) form via subsequent full oxidation of propene or by direct combustion of propane. The relative reactivity of propane and propene in this reaction scheme was determined by measuring the isotopic composition of products formed from unlabeled propene and [2-^{13}C]propane reactant mixtures (17–20). The isotopic content in reactants and products is shown in Fig. 1 for reactions on 15 wt% VO_x/ZrO_2. The ^{13}C fraction in propane

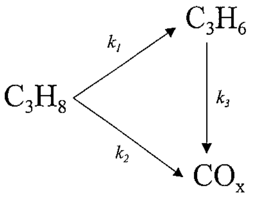

SCHEME 1. Reaction network in oxidative dehydrogenation of propane.

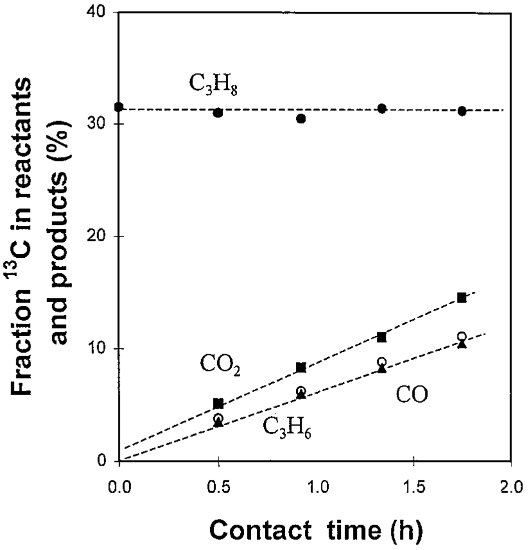

FIG. 1. ^{13}C content in reaction products of propene/[2-^{13}C]propane/O_2 mixtures on 15 wt% VO_x/ZrO_2 [593 K, 2.3 kPa [2-^{13}C]C_3H_8 0.5 kPa C_3H_6, 1.7 kPa O_2, balance He, gradientless batch reactor].

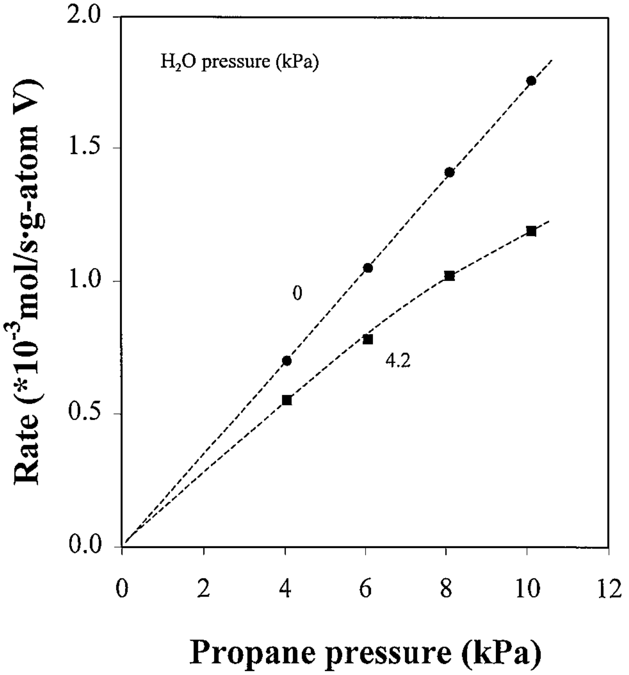

FIG. 2. Effect of C_3H_8 pressure on C_3H_6 formation rate at different H_2O concentrations on 10 wt% VO_x/ZrO_2 [605 K, 1.7 kPa O_2, balance He].

remained at its initial value (0.32). Thus, the isotopic content in propane is not diluted by propene hydrogenation, showing that the overall propane ODH reaction is irreversible at the conditions of our study. The ^{13}C fraction in propene increases with contact time, because [2-^{13}C]propene is increasingly formed via dehydrogenation of [2-^{13}C]propane. The ^{13}C fraction in CO and CO_2 also increases with contact time, but the ^{13}C content in CO is similar to that in propene at all contact times. The ^{13}C fraction in CO_2 is slightly higher than in CO or propene. This suggests that CO forms only via secondary oxidation of propene, but that CO_2 forms via both the secondary oxidation of propene and the direct combustion of propane. These results are consistent with the observed effects of reactor residence time on propene and CO_x selectivities (4, 5, 9–12).

3.2. Kinetic Dependence on C_3H_8, O_2, and H_2O

The effects of varying the concentrations of C_3H_8, O_2, and H_2O on the initial rate of propene formation were determined and similar kinetic rate expressions were obtained on bulk V_2O_5 and on VO_x/ZrO_2 with different VO_x loadings. Here, we show detailed data on 10 wt% VO_x/ZrO_2. Figure 2 shows propene formation rates as a function of propane partial pressure at a given value of O_2 partial pressure without added H_2O. Propene formation rates increase linearly with increasing propane partial pressure, in agreement with previous reports (10, 12, 21). The presence of H_2O (4.2 kPa) decreases ODH reaction rates and the apparent reaction order in propane (Fig. 2). Figure 3 shows that ODH rates are independent of O_2 partial pressure when H_2O is not present in the C_3H_8/O_2 feed, as reported previously (10–13). The presence of H_2O (4.2 kPa) leads to a small positive effect of O_2 partial pressure on the rate of propane ODH reactions. The effect of H_2O partial pressure on propane ODH rates is shown in Fig. 4 at constant C_3H_8 and O_2

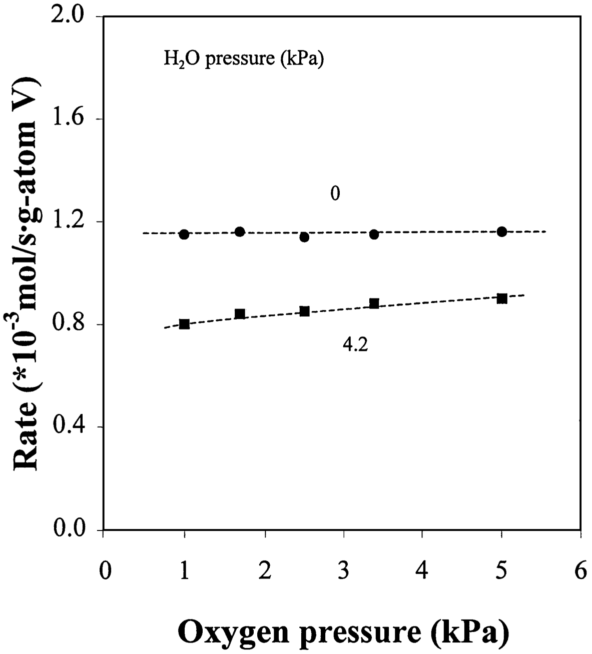

FIG. 3. Effect of O_2 pressure on C_3H_6 formation rate at different H_2O concentrations on 10 wt% VO_x/ZrO_2 [605 K, 6.7 kPa C_3H_8, balance He].

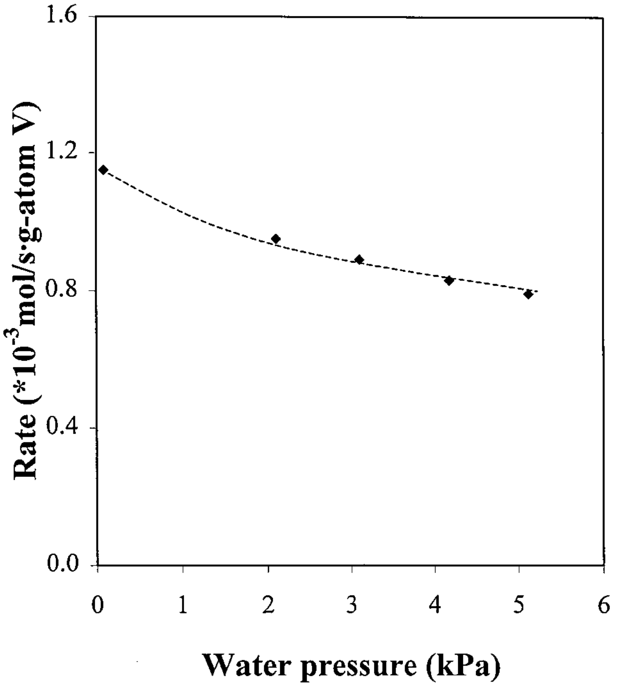

FIG. 4. Effect of H_2O pressure on C_3H_6 formation rate on 10 wt% VO_x/ZrO_2 [605 K, 6.7 kPa C_3H_8, 1.7 kPa O_2, balance He].

partial pressures. Water inhibits the rate of propane ODH, in a manner similar to that reported for ethane ODH reactions on V_2O_5-based catalysts (21).

3.3. *Analysis of Elementary Steps*

Several mechanistic sequences have been proposed for the ODH of propane (7, 8, 10–13). On V_2O_5 supported on amorphous $AlPO_4$, Andersson (8) proposed an Eley–Rideal mechanism in which gas phase propane reacts directly with O at the surface of the catalyst. Creaser *et al.* (11) suggested that propane reacts with lattice oxygen on the surface of V–Mg–O catalyst to form adsorbed propyl species, which then lose an additional H atom to form adsorbed propene. These authors concluded that the oxygen surface concentration is not in equilibrium with gas-phase O_2, but it is determined by the relative rates of oxygen chemisorption and of reaction with propane. Oyama (22) examined the relationship between adsorbate bonding and selectivity in partial oxidation on V_2O_5/SiO_2 and proposed that the ODH of ethane to form ethene proceeds via adsorbed ethyl intermediates bonded to one lattice oxygen on VO_x/SiO_2.

The observed dependence of propane ODH reaction rates on the concentration of reactants and products is consistent with a Mars–van Krevelen redox mechanism, in which irreversible C–H bond activation steps occur on VO_x surfaces exposing predominantly lattice oxygens and terminal hydroxyl groups. The following steps are required in order to complete a propane ODH turnover:

1. Weak adsorption of propane by interaction with lattice oxygen (O^*).

$$C_3H_8 + O^* \rightleftarrows C_3H_8O^* \qquad [1]$$

2. C–H bond activation by abstraction of a H atom from adsorbed propane using a neighboring oxygen atom.

$$C_3H_8O^* + O^* \rightarrow C_3H_7O^* + OH^* \qquad [2]$$

3. Desorption of propene by hydride elimination.

$$C_3H_7O^* \rightarrow C_3H_6 + OH^* \qquad [3]$$

4. Recombination of OH groups to form water and a reduced V center (*).

$$OH^* + OH^* \rightleftarrows H_2O + O^* + {}^* \qquad [4]$$

5. Reoxidation of V centers via dissociative chemisorption of O_2.

$$O_2 + {}^* + {}^* \rightarrow O^* + O^* \qquad [5]$$

In this scheme, O^* is a lattice oxygen in V=O or V–O–V structures, OH^* is a hydroxyl group in V–O–H, $C_3H_7O^*$ represents an adsorbed propyl bonded to V through an O atom (e.g., V–O–C_3H_7), and * represents a surface vacancy associated with either one V^{+3} or two V^{+4} atoms in the VO_x lattice. As we show below, the above mechanism for the ODH of propane is consistent with the kinetic rate expressions obtained on VO_x/ZrO_2 and on bulk V_2O_5 powders.

The assumption of pseudo-steady-state for all reaction intermediates leads to a complex rate expression, which can be made simpler by additional assumptions about the reversibility of specific elementary steps. Step 1 is expected to involve the initial nondissociative chemisorption of weakly bound propane. The low activation energy for such processes and the expected weak binding energy of molecularly adsorbed propane are likely to lead to quasi-equilibrated adsorption–desorption steps with an equilibrium constant K_1. Step 2 is assumed to be irreversible based on the results of C_3H_8–C_3D_8 exchange studies shown in Section 3.5. The recombination of OH groups is assumed to be reversible and almost quasi-equilibrated, based on the observed inhibition by H_2O, which would not be possible if step 4 were irreversible, and on the results of C_3H_8–D_2O experiments (Section 3.6). O_2 chemisorption is assumed to be irreversible based on the rate of isotopic exchange of $^{16}O_2$–$^{18}O_2$ mixtures during ODH reactions (Section 3.4). Su *et al.* (23) did not detect significant reduction of VO_x/ZrO_2 during isothermal treatments in 1% C_3H_8/He at 673 K. Thus, the concentration of vacancies (*) is expected to be smaller than those of (O^*) and (OH^*) during ODH reactions of

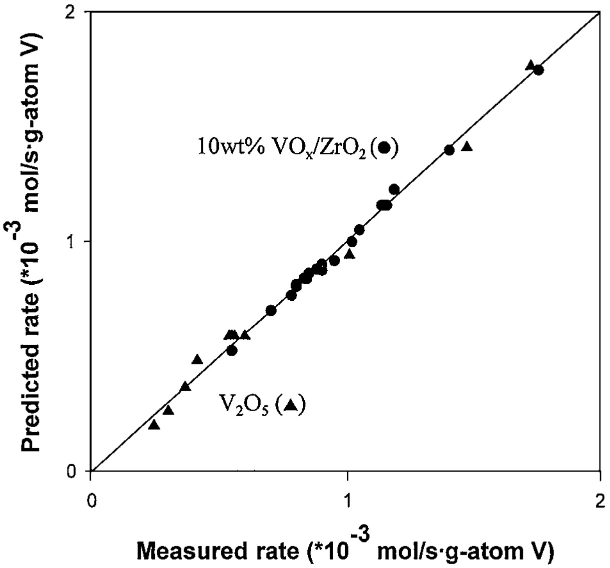

FIG. 5. Comparison of predicted (from Eq. [6]) and experimental C_3H_6 formation rates.

propane. These assumptions lead to the kinetic rate expression

$$r = k_2K_1[C_3H_8]/\\ \{1 + (K_4[H_2O])^{0.5}(k_2K_1[C_3H_8]/2k_5[O_2])^{0.25}\}^2, \quad [6]$$

where k_i is the rate coefficient and K_i is the equilibrium constant for reaction i. The rate of propane ODH reactions is first order in C_3H_8 concentration and zero order in the concentration of O_2 in the limit of very low H_2O concentrations. As the concentration of H_2O increases, propane ODH rates decrease and the apparent orders begin to deviate from those measured when the concentration of H_2O is very low. Figure 5 shows that the rates predicted by this expression at different C_3H_8, O_2, and H_2O concentrations are in excellent agreement with the experimental data obtained on both bulk V_2O_5 and VO_x/ZrO_2, confirming our previous proposals about the kinetic equivalence of VO_x species at the surfaces of polyvanadate domains and of bulk V_2O_5 (4). Alternate elementary steps, including propane interactions with surface vacancies and irreversible OH recombination steps did not give a rate expression in agreement with the experimental data. The next sections present the results of isotopic tracer studies designed to confirm the extent to which steps 1–5 are reversible during steady-state ODH reactions.

3.4. Irreversible Oxygen Dissociation and Involvement of Lattice Oxygen Atoms

The rate of propane ODH over VO_x/ZrO_2 exhibits a zero-order dependence on oxygen, suggesting that lattice oxygens are required for this reaction, as also proposed by others (14). The involvement of lattice oxygen atoms was confirmed by carrying out propane ODH reactions using $^{18}O_2$ on VO_x initially containing only ^{16}O and measuring the relative rates at which the two isotopes appear in the initial H_2O and CO_x products. Figure 6 shows the isotopic content of the H_2O formed during ODH of $^{18}O_2$–C_3H_8 mixtures on 15 wt% $V_2{}^{16}O_x/Zr^{16}O_2$ as the catalyst temperature was increased at a linear rate. The water formed initially is predominantly $H_2{}^{16}O$, indicating that C_3H_8 reacts predominantly with ^{16}O surface atoms that are part of the $V^{16}O_x$ lattice. As the catalyst temperature increases, the amount of $H_2{}^{18}O$ increases because ^{16}O in the lattice is gradually replaced by ^{18}O from $^{18}O_2$. At high temperatures, $H_2{}^{18}O$ becomes the most abundant isotopomer, because most of the initial ^{16}O in the VO_x lattice has been replaced by ^{18}O from O_2.

The reversibility of dissociative O_2 chemisorption was determined using an $^{18}O_2$–$^{16}O_2$–C_3H_8 reactant mixture by measuring the rate of appearance of mixed $^{18}O^{16}O$ isotopomers in the gas phase. Reversible dissociative chemisorption of O_2 would lead to rapid isotopic equilibration of $^{16}O_2$ and $^{18}O_2$ during propane ODH reactions, while irreversible chemisorption should preserve the initial bimodal isotopic distribution of $^{16}O_2$ and $^{18}O_2$ in the feed. Figure 7 shows the rate of product formation when $^{16}O_2$–$^{18}O_2$–C_3H_8 mixtures are reacted on 15 wt% $V_2{}^{16}O_x/Zr^{16}O_2$ as the temperature is increased at a linear rate. Products become detectable at about 550 K and increase in concentration with temperature until O_2 is depleted at about 700 K. C_3H_6, CO, CO_2, and H_2O formed during the reaction of propane, but $^{16}O^{18}O$ was not detected and the rates of $^{16}O_2$ and $^{18}O_2$ consumption were identical (Fig. 7b). Once $^{16}O_2$ is removed

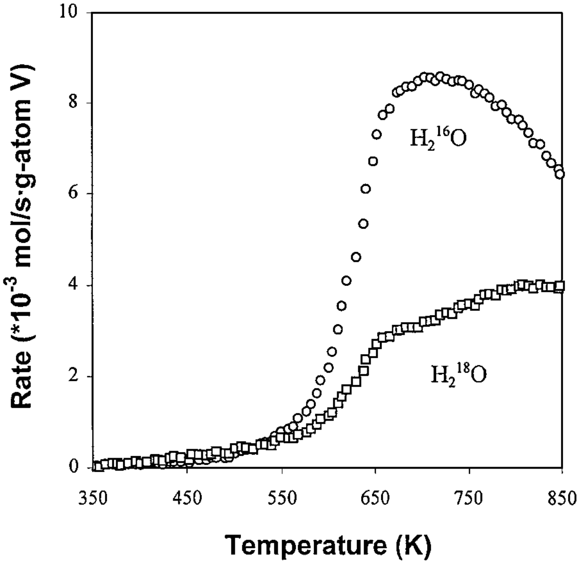

FIG. 6. H_2O formation rate from reactions of $^{18}O_2$–C_3H_8 mixtures on 15 wt% $V_2{}^{16}O_x/Zr^{16}O_2$ as a function of catalyst temperature.

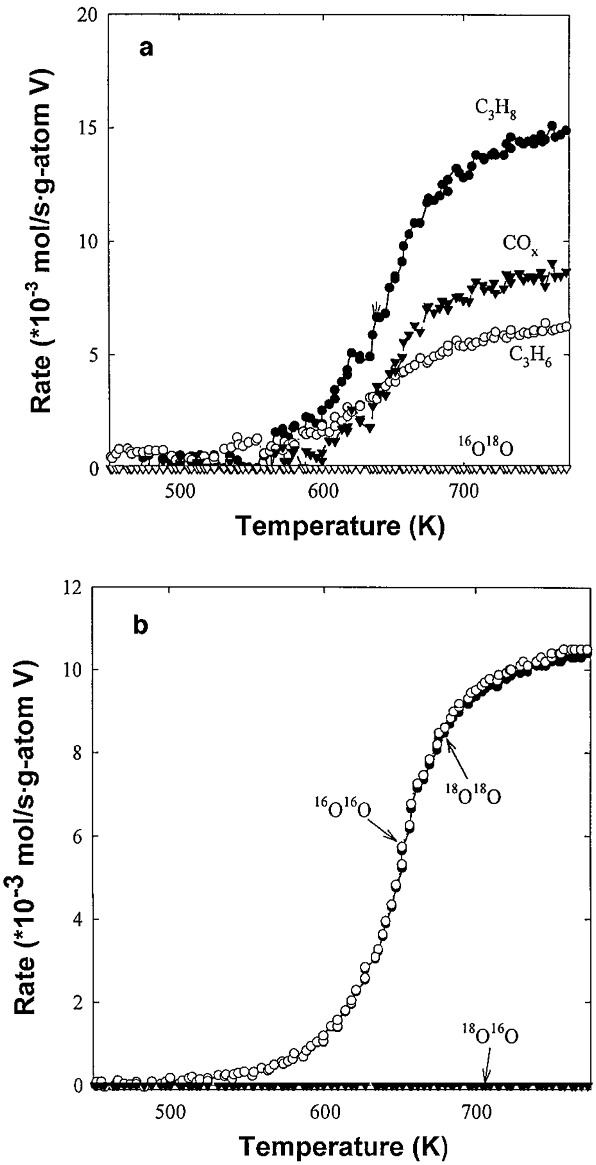

FIG. 7. (a) C_3H_8 consumption rate and C_3H_6, CO_x, and $^{16}O^{18}O$ formation rates from $^{18}O_2$–$^{16}O_2$–C_3H_8 mixtures on 15 wt% $V_2{}^{16}O_x/Zr^{16}O_2$ as a function of temperature. (b) $^{18}O_2$ and $^{16}O_2$ consumption rates, and $^{16}O^{18}O$ formation rates during reactions of $^{18}O_2$–$^{16}O_2$–C_3H_8 mixtures on 15 wt% $V_2{}^{16}O_x/Zr^{16}O_2$ as a function of temperature.

from the lattice, it is replaced in equivalent amounts from $^{16}O_2$ and $^{18}O_2$. The absence of $^{16}O^{18}O$ in the gas phase shows that the dissociative O_2 chemisorption step (step 5) required for propane ODH is irreversible at 605 K.

3.5. Irreversible Initial C–H Bond Activation in Propane

At very low H_2O concentrations, the rate of propene formation is first order in C_3H_8, suggesting that propane activation is a kinetically relevant step. The reversibility of C–H bond activation steps can be probed by measuring the rate of H–D isotopic scrambling in "unreacted" propane during reactions of C_3H_8/C_3D_8–O_2 mixtures (17, 18, 20). If the C–H bond activation step is reversible, $C_3H_xD_{8-x}$ $(0 < x < 8)$ isotopomers will form via the microscopic reverse of the C–H bond activation step (17, 18). If C–H bond activation is irreversible, the rate of formation of $C_3H_xD_{8-x}$ $(0 < x < 8)$ isotopomers will be much lower than the rate of propane conversion to propene and CO_x.

Figure 8 shows the deuterium distribution in propane during the reaction of a $C_3H_8/C_3D_8/O_2$ mixture on 4 wt% VO_x/ZrO_2 at about 4% propane conversion. At all chemical conversions, the deuterium distribution in the remaining propane is identical to the bimodal undeuterated and perdeuterated distribution present in the propane reactants. No cross-exchange products were detected by mass spectrometry, suggesting that C–H bond activation is an irreversible step in the ODH reaction sequence. The isotopomer distributions were determined by matrix methods that neglect secondary kinetic isotope effects in the fragmentation process (16). This procedure can lead to slightly negative mole fractions for some of the isotopomers (see C_3D_7H in Fig. 8). The mole fractions of all mixed propane isotopomers are zero within the accuracy of the measurements and of the deconvolution procedures.

The kinetic relevance of C–H (and C–D) bond dissociation steps can be inferred from the effect of deuterium substitution on the rate of propene and CO_x formation. The reaction rate constants for ODH reactions of undeuterated (C_3H_8) and perdeuterated (C_3D_8) propane (k_{C-H} and k_{C-D}, respectively) were obtained from the initial rates of propene formation from C_3H_8–O_2 and C_3D_8–O_2 mixtures. Kinetic isotope effects for propane direct combustion and for secondary propene combustion reactions can also be

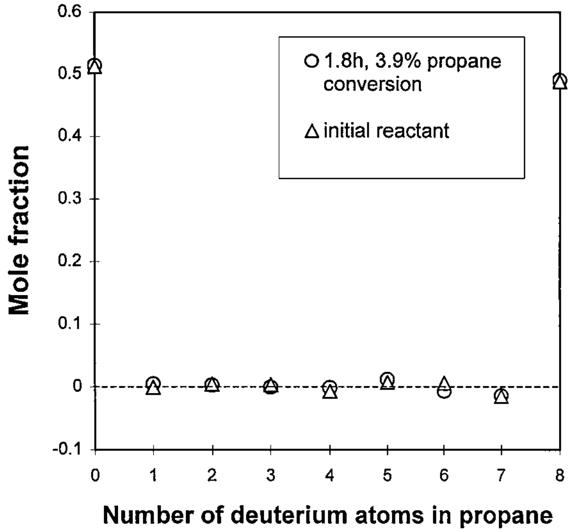

FIG. 8. Deuterium cross exchange for $C_3H_8/C_3D_8/O_2$ reactant mixture on 4 wt% VO_x/ZrO_2. Deuterium distributions in reactant mixture and in "unreacted" propane [593 K, 7.1 kPa C_3H_8, 7.1 kPa C_3D_8, 1.7 kPa O_2, balance He, gradientless batch reactor].

measured from the initial rates of CO_x formation and from the effect of residence time on propene selectivity for C_3H_8–O_2 and C_3D_8–O_2 mixtures.

An analysis of the kinetic isotope effects requires that we treat the system using the reaction network of Scheme 1. At relatively low conversions and without the external addition of water, the rate of each of these reactions is well described by

$$r_1 = k_1'[C_3H_8] \tag{7}$$

$$r_2 = k_2'[C_3H_8] \tag{8}$$

$$r_3 = k_3'[C_3H_6], \tag{9}$$

where k_i' is the apparent first-order rate coefficient for reaction i. The propene selectivity at relatively low conversions in a batch reactor is given by (5)

$$S = S^0(1 - k_3'C_vt/2), \tag{10}$$

where C_v is concentration of V atoms per unit reactor volume, t is the reaction time in the batch reactor, and $S^0 = k_1'/(k_1' + k_2')$ is the initial propene selectivity (as t goes to zero). The initial rate of propene conversion (as $t \rightarrow 0$) gives the value of k_1'. The initial propene selectivity (S^0) depends on the k_1'/k_2' ratio which can then be used to calculate k_2'. Finally, k_3' is obtained from the dependence of selectivity on time predicted by Eq. [10].

The rate constants $k_{i,\mathrm{C-H}}'$, $k_{i,\mathrm{C-D}}'$ and ratios measured on 4 wt% VO_x/ZrO_2 are listed in Table 1. The kinetic isotope effect (defined as $k_{i,\mathrm{C-H}}'/k_{i,\mathrm{C-D}}'$ ratio) is greater than unity for all reactions, suggesting the involvement of C–H bonds in kinetically relevant steps. Propane ODH and propene combustion show similar kinetic isotope effects (2.5, 2.2) consistent with the assumption that the initial C–H bond activation step limits the rates of both reactions and that the two reactions require similar surface oxygen species. Propane combustion reactions show a slightly lower kinetic isotope effect (1.7). Grasselli *et al.* (12) measured the kinetic isotope effect for the oxidation of propane and propene on nickel–cobalt–molybdates. They reported kinetic isotope effects of 1.7 for propane and 1.9 for propene oxidation (at 773 K) and they reached similar conclusions about the similarity in rate-determining steps for these two reactions.

TABLE 1

Reaction Rate Constant k_1', k_2', and k_3' ($cm^3\ mol^{-1}\ s^{-1}$) on 4 wt% VO_x/ZrO_2 Catalysts

	Primary dehydrogenation (k_1')	Primary combustion (k_2')	Secondary combustion (k_3')
$k_{i,\mathrm{C-H}}'$	185	103	3360
$k_{i,\mathrm{C-D}}'$	74	60	1520
$k_{i,\mathrm{C-H}}'/k_{i,\mathrm{C-D}}'$	2.5	1.7	2.2

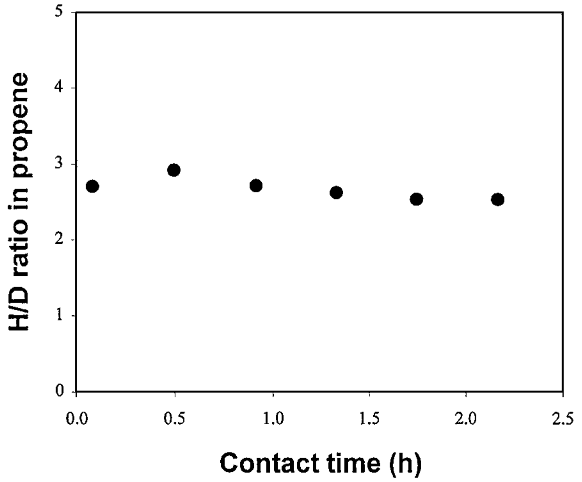

FIG. 9. H/D ratio in propene formed from $C_3H_8/C_3D_8/O_2$ mixtures on 4 wt% VO_x/ZrO_2 [593 K, 7.1 kPa C_3H_8, 7.1 kPa C_3D_8, 1.7 kPa O_2, balance He, gradientless batch reactor].

H/D ratios in the propene formed from $C_3H_8/C_3D_8/O_2$ mixtures provide confirming data for the relative rates of C–H and C–D bond activation. The H/D ratio in the reactant mixture is approximately 1, but propene products have an H/D ratio of 2.7 on 4 wt% VO_x/ZrO_2 at all contact times between 0.1 and 2 h (O_2 conversions of 5% to 95%) (Fig. 9). This value is almost identical to the value obtained for the kinetic isotope effect (2.5) on this catalyst from independent measurements of the rates of propene formation from C_3H_8–O_2 and C_3D_8–O_2 mixtures (Table 1). The binomial deuterium distribution (Fig. 10) observed in propene at all chemical conversions shows that H is mobile on the catalyst

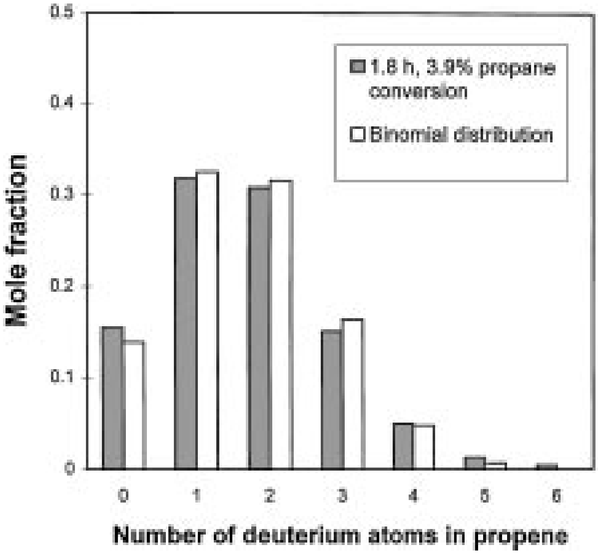

FIG. 10. Deuterium distribution in propene formed from $C_3H_8/C_3D_8/O_2$ mixtures on 4 wt% VO_x/ZrO_2 [593 K, 7.1 kPa C_3H_8, 7.1 kPa C_3D_8, 1.7 kPa O_2, balance He, gradientless batch reactor].

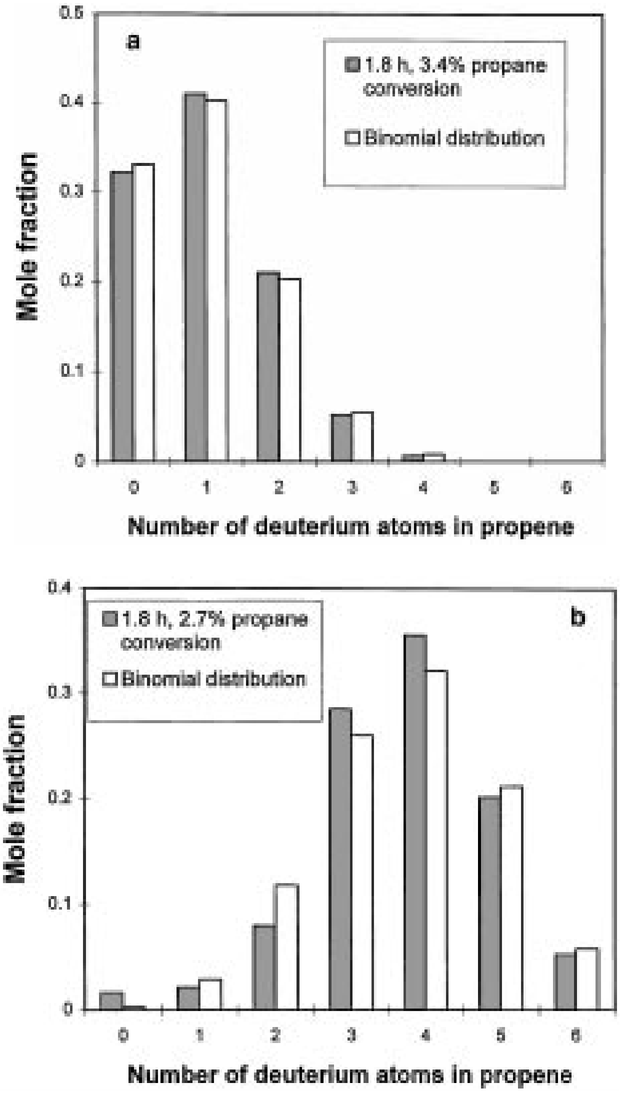

FIG. 11. (a) Deuterium distribution in propene formed from C_3H_8/D_2O/O_2 mixtures on 4 wt% VO_x/ZrO_2 [593 K, 14.2 kPa C_3H_8, 0.5 kPa D_2O, 1.7 kPa O_2, balance He, gradientless batch reactor]. (b) Deuterium distribution in propene formed from C_3D_8/H_2O/O_2 mixtures on 4 wt% VO_x/ZrO_2 [593 K, 14.2 kPa C_3D_8, 0.5 kPa H_2O, 1.7 kPa O_2, balance He, gradientless batch reactor].

surface and that multiple exchange of C_3H_6 and C_3D_6 with the surface H/D pool occurs rapidly during propane ODH reactions.

3.6. Reversible Recombinative Desorption of OH Groups to Form Water

Water is a product of propane ODH reactions and it inhibits propane ODH (Figs. 2–4), suggesting that water desorption is reversible. This effect of water is similar to that reported by Oyama *et al.* (21) for ethane ODH reactions on V_2O_5/SiO_2. The reversibility of the recombinative desorption of OH groups to form water was determined by measuring the deuterium distribution in the propene formed from $C_3H_8/D_2O/O_2$ and $C_3D_8/H_2O/O_2$ mixtures on 4 wt% VO_x/ZrO_2. For both mixtures, no $C_3H_xD_{8-x}$ $(0 < x < 8)$ isotopomers were detected in the unreacted propane even after a contact time of 2 h (ca. 4% propane conversion), confirming that propane C–H bond activation steps are irreversible. However, binomial deuterium distributions in the propene formed from $C_3H_8/D_2O/O_2$ and $C_3D_8/H_2O/O_2$ mixtures were detected at all contact times (Figs. 11a and 11b). These data suggest that water can dissociatively adsorb on the catalyst surface during ODH reactions (i.e., OH recombination to form water is reversible). They also suggest that H atoms on the surface are mobile and that multiple exchange of C_3H_6 and C_3D_6 with the surface H/D pool present as hydroxyl groups occurs during propane ODH reactions. These results are consistent with the assumption of quasi-equilibrated recombinative desorption of OH groups (reaction 4), which was used in order to describe quantitatively the observed inhibition effects of water on propane ODH reaction rates.

4. CONCLUSIONS

Oxidative dehydrogenation of propane on VO_x/ZrO_2 and on bulk V_2O_5 powders occurs via parallel and sequential reactions. Propene is the most abundant primary product. CO and CO_2 form via secondary combustion of propene, and CO_2 forms also by direct combustion of propane. The dependences of reaction rates on C_3H_8, O_2, and H_2O concentrations are identical on supported VO_x and on V_2O_5 powders, suggesting that similar active centers are present on both surfaces. The reaction kinetics are consistent with a Mars–van Krevelen redox sequence in which lattice oxygen atoms participate in the irreversible activation of C–H bonds in propane. The resulting alkyl species desorb as propene and the remaining OH groups recombine to form water and reduced V centers. These reduced V centers reoxidize by irreversible dissociative chemisorption of O_2. The recombination of OH groups to form water is reversible. The assumption that surface oxygen and OH groups are the most abundant surface intermediates leads to a rate expression that describes accurately the measured kinetics of propane ODH reactions. Isotopic tracer studies fully confirmed the assumptions required in order to describe the observed effects of reactant and product concentrations on the rate of propane ODH reactions.

ACKNOWLEDGMENTS

This work was supported by the Director, Office of Basic Energy Sciences, Chemical Sciences Division of the U.S. Department of Energy under Contract DE-AC03-76SF00098.

REFERENCES

1. Blasko, T., and López Nieto, J. M., *Appl. Catal. A* **157**, 117 (1997).
2. Kung, H. H., *Adv. Catal.* **40**, 1 (1994).
3. Albonetti, S., Cavani, F., and Trifiro, F., *Catal. Rev.-Sci. Eng.* **38**, 413 (1996).
4. Khodakov, A., Olthof, B., Bell, A. T., and Iglesia, E., *J. Catal.* **181**, 205 (1999).
5. Khodakov, A., Yang, J., Su, S., Iglesia, E., and Bell, A. T., *J. Catal.* **177**, 343 (1998).
6. Centi, G., and Triffiro, F., *Appl. Catal. A* **143**, 3 (1996).
7. Mamedov, E. A., and Cortés-Corberan, V., *Appl. Catal. A* **127**, 1 (1995).
8. Andersson, S. L. T., *Appl. Catal. A* **112**, 209 (1994).
9. Michaels, J. N., Stern, D. L., and Grasselli, R. K., *Catal. Lett.* **42**, 135 (1996).
10. Michaels, J. N., Stern, D. L., and Grasselli, R. K., *Catal. Lett.* **42**, 139 (1996).
11. Creaser, D., and Andersson, B., *Appl. Catal. A* **141**, 131 (1996).
12. Stern, D. L., and Grasselli, R. K., *J. Catal.* **167**, 560 (1997).
13. Sautel, M., Thomas, G., Kaddouri, A., Mazzocchia, C., and Anouchinsky, R., *Appl. Catal. A* **155**, 217 (1997).
14. Boisdron, N., Monnler, A., Jalowiecki-Duhamel, L., and Barbaux, Y., *J. Chem. Soc. Faraday Trans.* **91**, 2899 (1995).
15. Iglesia, E., Baumgartner, J. E., and Price, G. L., *J. Catal.* **134**, 549 (1992).
16. Price, G. L., and Iglesia, E., *Ind. Eng. Chem. Res.* **28**, 839 (1989).
17. Biscardi, J. A., and Iglesia, E., *Catal. Today* **31**, 207 (1996).
18. Biscardi, J. A., and Iglesia, E., *J. Catal.* **182**, 117 (1999).
19. Iglesia, E., and Baumgartner, J. E., *Catal. Lett.* **21**, 55 (1993).
20. Meitzner, G. D., Iglesia, E., Baumgartner, J. E., and Huang, E. S., *J. Catal.* **140**, 209 (1993).
21. Oyama, S. T., Middlebrook, A. M., and Somorjai, G. A., *J. Phys. Chem.* **94**, 5029 (1990).
22. Oyama, S. T., *J. Catal.* **128**, 210 (1991).
23. Su, S. C., and Bell, A. T., *J. Phys. Chem. (B)* **102**, 7000 (1998).